International Journal of Thermal Sciences 149 (2020) 106199

Contents lists available at ScienceDirect

International Journal of Thermal Sciences

journal homepage: http://www.elsevier.com/locate/ijts

Manipulation of bubble migration through thermal capillary effect under variable buoyancy

Yang Ma [a], Yongpan Cheng [a,b,*], Yang Shen [a], Jinliang Xu [a,b,**], Yi Sui [c]

[a] Beijing Key Laboratory of Multiphase Flow and Heat Transfer for Low Grade Energy, North China Electric Power University, Beijing 102206, China
[b] Key Laboratory of Power Station Energy Transfer Conversion and System of Ministry of Education, North China Electric Power University, Beijing 102206, China
[c] School of Engineering and Materials Science, Queen Mary University of London, Mile End Road, London, E1 4NS, United Kingdom

ARTICLE INFO

Keywords:
Bubble migration
Manipulation
Thermal capillary effect
Variable buoyancy

ABSTRACT

The spontaneous bubble migration and the active manipulation have widely applications in outer space. In this paper, the bubble migration driven by the thermal capillary effect is numerically investigated under variable buoyancy. The numerical model is built up through the transient two-dimensional axisymmetric model with a level set method. It is found that the magnitude and direction of bubble migration velocity is determined by the competition of upward buoyant effect and downward thermal capillary effect. These two effects can be controlled by changing the ratios of density, viscosity, thermal conductivity of bubble over surrounding liquid, as well as Reynolds number, Froude number, Peclet number and Marangoni number. With increasing Froude number or decreasing density ratio, the thermal capillary effect becomes dominant over the buoyant effect, the bubble will migrate from upward to downward. The Marangoni number has negligible effect on the bubble migration at low Reynolds numbers, while at high Reynolds numbers, increasing Marangoni number can reduce the upward migration velocity due to stronger thermal capillary effect. At low Reynolds numbers, with the increasing ratios of viscosity and thermal conductivity, the downward driving force is increased, while at high Reynolds numbers, the ratios have negligible effect on the bubble migration. These findings may provide the guidance for actively manipulating the bubbles under variable buoyancy.

1. Introduction

Active manipulation of the bubble/droplet has wide application in the outer space, such as material processing in the reduced gravity environment, recycling of life-sustaining substances such as water and oxygen in long duration space excursions [1]. Thermal capillary effect is caused by the uneven distribution of surface tension due to temperature gradient. Under normal gravity the thermal capillary force may be suppressed by the buoyant force, while under reduced gravity it can be comparable with the buoyant force, or even becomes dominant. The early development on bubble/droplet migration due to thermal capillarity under microgravity has been reviewed by Subramanian and Balasubramaniam [2]. Young et al. [3] firstly studied the bubble migration in the liquid column with applied temperature gradient, and they also derived the analytical solution on bubble migration velocity under combined thermal capillary and buoyant forces, in which the momentum and energy transport were negligible. Balasubramaniam and Chai [4] proved that the analytical solution was still applicable under any Reynolds number only if Marangoni number is far less than 1. Crespo et al. [5] extended the study to large Reynolds number and arbitrary Marangoni numbers. Crespo and Jimenez-Fernandez [6] provided the expressions for bubble migration velocity at infinite large Reynolds number and Marangoni numbers.

Through experiment Hadland et al. [7] studied thermal capillary migration of bubbles in NASA space shuttle mission. In their experiments, air bubbles were injected into a cavity filled with silicone oil, and the temperature gradient remained on the opposite wall. The bubbles were found to move from the cold plate to the hot plate due to Marangoni convection. Szymczyk et al. [8] injected droplets and bubbles into silicone oil respectively in their space experiments in NASA Aerospace Laboratory. The migration velocity of bubbles is close to that of

* Corresponding author. Beijing Key Laboratory of Multiphase Flow and Heat Transfer for Low Grade Energy, North China Electric Power University, Beijing 102206, China.
** Corresponding author. Beijing Key Laboratory of Multiphase Flow and Heat Transfer for Low Grade Energy, North China Electric Power University, Beijing 102206, China.
E-mail addresses: chengyp@ncepu.edu.cn (Y. Cheng), xjl@ncepu.edu.cn (J. Xu).

https://doi.org/10.1016/j.ijthermalsci.2019.106199
Received 16 July 2019; Received in revised form 21 November 2019; Accepted 21 November 2019
Available online 28 November 2019
1290-0729/

Nomenclature

Ca	Capillary number
C_p^*	Non-dimensional specific heat
F	Non-dimensional force
Fr	Froude number
g	Gravitational acceleration
H	Heaviside function
K_{Is}	Multiplier
Ma	Marangoni number
p	Non-dimensional pressure
Pe	Peclet number
Pr	Prandtl number
r_0	Bubble radius
R_{c}	Ratio of the thermal conductivity, $R_{\mathrm{c}} = \lambda_l/\ \lambda_{\mathrm{g}}$
R_{C_p}	Ratio of the specific heat $R_{C_p} = C_{p,\mathrm{l}}/C_{p,g}$
R_{d}	Ratio of the density, $R_{\mathrm{d}} = \rho_{\mathrm{l}}/\rho_{\mathrm{g}}$
R_{v}	Ratio of the dynamic viscosity, $R_{\mathrm{v}} = \mu_{\mathrm{l}}/\mu_{\mathrm{g}}$
Re	Reynolds number
t	Non-dimensional time
T	Non-dimensional temperature
u_0	Characteristic velocity
u,v	Non-dimensional velocity
x,y	Non-dimensional coordinates

Greek symbols

ε	Interface thickness
φ	Distance function
δ	Dirac delta function
κ	Non-dimensional curvature
λ^*	Non-dimensional thermal conductivity
μ^*	Non-dimensional dynamic viscosity
ρ^*	Non-dimensional density
σ_0	Surface tension
σ_T	Variation coefficient of surface tension over temperature

Subscript

B	Buoyant
g	Gas
P	Pressure
In	Inertial
l	Liquid
m	Migration
Tc	Thermal Capillary
Vis	Viscosity

numerical simulation. Thompson et al. [9] explored the movement of nitrogen bubbles in the falling tower. They studied the thermal capillary migration velocity under different temperature gradients in liquid. The experimental results are qualitatively consistent with the results, which are predicted by the linear theory by ignoring the Reynolds number and Marangoni number. Balasumbramaniam et al. [1] studied the motion of a single bubble in silicone oil at a given temperature gradient under weakened gravity. The experimental results show that the dimensionless migration velocity decreases with the increase of the Marangoni number and approaches the theoretical solution of the limit of large Marangoni numbers.

Due to the great difficulties of experimental time and cost under microgravity, especially for studies at large Reynolds or Marangoni numbers, the numerical study provides a cost-effective way for bubble migrations. Szymczyk et al. [10] used a two-dimensional model to simulate the bubble migration under the conditions of non-zero *Re* number and large Ma number. The numerical simulation study of Balasubramaniam and Lavery [11] shows that the scaled migration velocity of the bubbles is less affected by the Reynolds number, while it is greatly affected by the Marangoni number. Ma et al. [12] found that the bubble migration velocity is independent of the Marangoni number at fairly large Marangoni number. Zhang et al. [13] adopted the modified lattice Boltzmann method to study the bubble migration under microgravity, and found that the floating vapor bubble moves towards the hot wall due to the Marangoni convection along the liquid-vapor interface. Zhao et al. [14] adopted the level-set method and the continuum interface model to simulate the thermocapillary migration of a deformable droplet, the numerical results agree quite well with the experimental data in space. Furthermore, it is found that the terminal migration velocity decreases monotonously with the increasing Marangoni number, the topological flow structure and temperature fields are also obtained. Besides the temperature gradient, the thermal radiation can also cause the uneven temperature distribution around the bubbles. Zhang et al. [15] studied the thermal capillary migration of bubble/droplet under thermal radiation, and obtained the variation of bubble/droplet migration velocity under different Reynolds numbers and physical properties of bubble/droplet. Tripathi et al. [16] studied the bubble motion in a tube with non-uniformly heated walls containing self-rewetting fluid, the surface tension of the fluid exhibits a parabolic dependence on temperature. It is found that with the buoyance and thermal capillary, the bubble can arrive at certain location of the tube. Then Balla et al. [17] extended to study the three-dimensional effect of the bubble in the self-rewetting fluid in the channel.

From the literature review above, it can be seen that most of the studies are focused on the bubble/droplet migration when the thermal capillary effect is dominant over the buoyant effect. In this paper, the focus is given to the critical condition when the thermal capillary effect and buoyant effect are equivalent. Under this condition the interaction between two effects becomes very important, they can determine both the magnitude and direction of the migration velocity, hence this is of great significance in actively manipulating the bubble migration direction and magnitude. The active manipulation method of bubble migration in the liquid is explored by changing the capillary, viscous, gravity and thermal capillary forces as well as the physical properties in terms of non-dimensional parameters.

In the following sections, the physical models and mathematical formulation are introduced first. Then the reliability of the numerical model is verified by an analytical solution with thermal capillary effect and buoyant effect. The numerical simulation is extended to the bubble migration under the combined effect of thermal capillarity and buoyancy. The effects of density ratio, thermal conductivity ratio and viscosity ratio on the migration velocity are studied under different Froude numbers at both low and high Reynolds numbers. Finally, some conclusions are drawn for active manipulation of bubble migration under the critical condition when the thermal capillary effect and buoyant effect are equivalent.

2. Physical model and mathematical formulation

Fig. 1 is the schematic diagram for thermal capillary migration of bubble under buoyancy. The downward temperature gradient is imposed across the bubble, resulting in the upward thermal capillary force along the gas-liquid interface, then the induced pressure drop will drive the bubble to move downward. In the meantime, the buoyant force will drive the bubble to move upward. The thermal capillary force will compete with the buoyant force, and determine the magnitude and direction of migration velocity of the bubble. When the thermal capillary force is dominant, the bubble will move downward; while when the

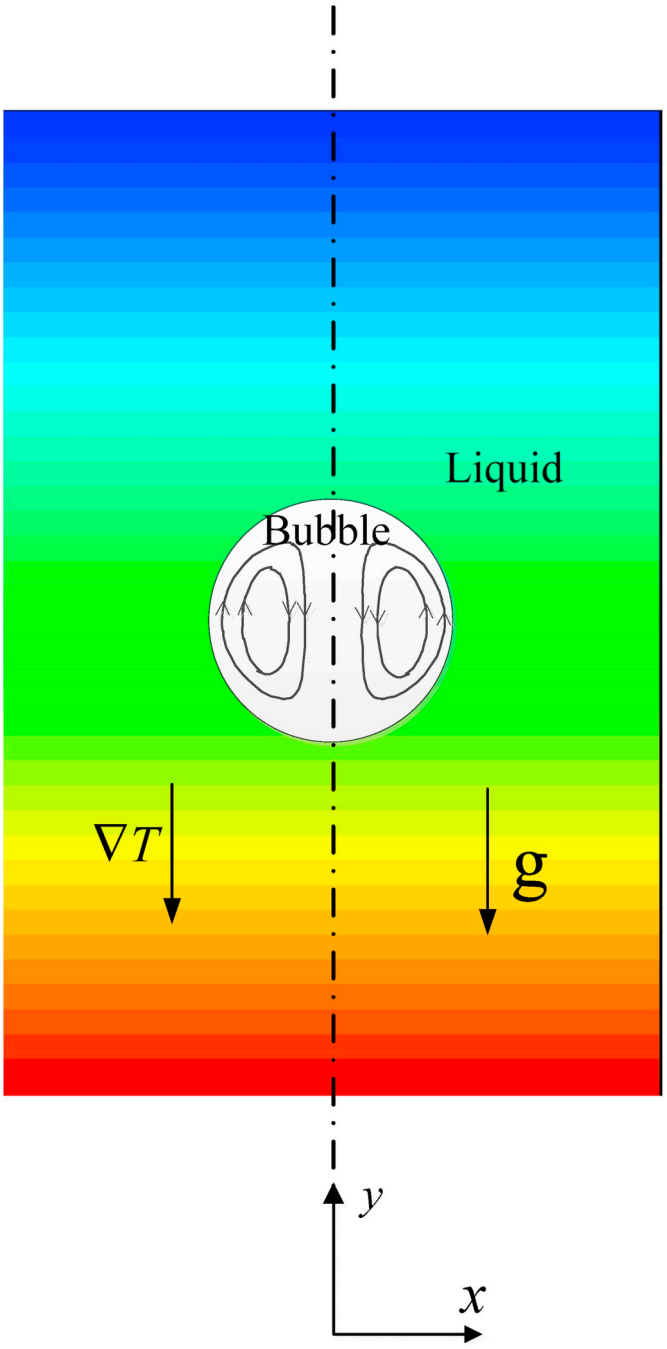

Fig. 1. Schematic diagram of bubble migration under both the thermal capillary force and buoyant force.

buoyant force is dominant, the bubble will move upward. By adjusting the relative magnitude of thermal capillary force and buoyant force, the bubble migration can be manipulated.

The characteristic velocity is defined based on thermal-capillary force

$$u_0 = \frac{\sigma_T r_0 \nabla T}{\mu_l} \tag{1}$$

The characteristic length is the bubble radius r_0, and the characteristic temperature difference is the temperature gradient over the bubble radius $r_0\nabla T$. Then the non-dimensional governing equations for bubble migration under thermal capillary force and buoyant force are as follows [15]:

The continuity equation

$$\nabla \cdot \vec{u} = 0 \tag{2}$$

The momentum equation

$$\frac{\partial \vec{u}}{\partial t} + \vec{u}\cdot\nabla\vec{u} = -\frac{1}{\rho^*}\nabla p + \frac{1}{\rho^* \mathrm{Re}}\nabla\cdot\left[\mu^*\left(\nabla\vec{u} + \nabla\vec{u}^T\right)\right] + \frac{1 - \mathrm{Ma}\cdot T}{\rho^* \mathrm{Re}\cdot\mathrm{Ca}}\kappa\vec{n}\delta(\varphi) - \frac{\mathrm{Ma}}{\rho^* \mathrm{Re}\cdot\mathrm{Ca}}\nabla_s T\delta(\varphi) + \frac{(R_d - 1)}{\rho^* R_d \mathrm{Fr}^2}\vec{j} \tag{3}$$

The first term in the source terms is the surface tension in the normal direction of the interface, the second term is the thermal capillary force in the tangential direction along the interface, and the third term is the buoyant force on the bubble.

The energy equation

$$\frac{\partial T}{\partial t} + \vec{u}\cdot\nabla T = \frac{1}{\rho^* C_p^* \mathrm{Re}\cdot\mathrm{Pr}}\nabla\cdot(\lambda^*\nabla T) \tag{4}$$

The transient axisymmetric level set method is adopted to capture the gas-liquid interface evolution.

The level set function is solved from the level set convection equation to track the interface

$$\frac{\partial \varphi}{\partial t} + u\cdot\nabla\varphi = 0 \tag{5}$$

The non-dimensional physical properties are defined based on the values of liquid as follows:

$$\rho^* = (1 - H) + H/R_\mathrm{d} \tag{6a}$$

$$\mu^* = (1 - H) + H/R_\mathrm{v} \tag{6b}$$

$$\lambda^* = (1 - H) + H/R_\mathrm{c} \tag{6c}$$

$$C_p^* = (1 - H) + H/R_{C_p} \tag{6d}$$

Here H is the Heaviside function [18].

$$H_\varepsilon(\varphi) = \begin{cases} 0 & \varphi < -1.5dx \\ \frac{1}{2}\left[1 + \frac{\varphi}{\varepsilon} + \frac{1}{\pi}\sin\left(\frac{\pi\varphi}{\varepsilon}\right)\right] & |\varphi| \le 1.5dx \\ 1 & \varphi > 1.5dx \end{cases} \tag{7}$$

The non-dimensional parameters are based on the physical properties in the liquid region as follows:

Reynolds number

$$\mathrm{Re} = \frac{\rho_l u_0 r_0}{\mu_l} \tag{8a}$$

Capillary number

$$\mathrm{Ca} = \frac{\mu_l u_0}{\sigma_0} \tag{8b}$$

Froude number

$$\mathrm{Fr} = \frac{u_0}{\sqrt{g r_0}} \tag{8c}$$

Effective Marangoni number

$$\mathrm{Ma} = \frac{\sigma_T r_0 \nabla T}{\sigma_0} \tag{8d}$$

The bubble is assumed as spherical and stationary initially. Due to the symmetry for bubble migration in y direction, only the right half of the bubble is simulated, the two-dimensional axisymmetric model is adopted, which greatly reduces the complexity of numerical simulation. The standard project method is adopted to solve the coupling between

the continuity equation and momentum equation. The Adams-Bashforth scheme and Crank-Nicolson schemes are adopted to solve the advection term and diffusion term respectively. The central difference scheme is adopted to discretize the spatial terms. After sensitivity checking, the mesh size is chosen as 101×301, the computational domain is 4×12 and the time step 1×10^{-4}. The convergence criterion for each time step is that the residues of the continuity equation and the energy equation are less than 1×10^{-3}. The default settings are $\mathrm{Re} = 2$, $\mathrm{Ca} = 0.1$, $\mathrm{Pr} = 1.0$ and the ratio of physical properties of the outer liquid and inner bubble are $R_d = R_v = R_c = R_{Cp} = 1$.

The left boundary is axisymmetric condition, and the other boundaries are free boundary condition, as follows:

Left boundary ($x = 0$)

Symmetric: $u = 0, \frac{\partial v}{\partial x} = 0, \frac{\partial T}{\partial x} = 0$

Right boundary ($x = 4$)

Free boundary: $v = 0, \frac{\partial u}{\partial x} = 0, \frac{\partial T}{\partial x} = 0$

Lower boundary ($y = 0$)

Free boundary: $u = 0, \frac{\partial v}{\partial y} = 0, \frac{\partial T}{\partial y} = 0$

Upper boundary ($y = 12$)

Free boundary: $u = 0, \frac{\partial v}{\partial y} = 0, \frac{\partial T}{\partial y} = 0$

3. Results and discussion

3.1. Numerical validation

In order to validate the current numerical model, the numerical results are compared with the analytical solution. The analytical solution for migration velocity under thermal capillary effect in viscous Stokes flow is provided by Young et al. [3]. The characteristic velocity u_0 is defined based on the thermal capillary force in Eq. (1). After normalization, the non-dimensional migration velocity under thermal capillary force in viscous flow with downward temperature gradient is as follows:

$$u_m = \frac{-2}{\left(2 + 3\frac{1}{R_v}\right)\left(2 + \frac{1}{R_c}\right)} \tag{9}$$

From Eq. (9) it can be seen that the migration velocity under thermal capillary effect only depends on the viscosity ratio R_v and thermal conductivity ratio R_c. In Fig. 2(a) the numerical results are compared with the analytical solutions under different viscosity ratios at thermal conductivity ratio $R_c = 1$ at low Reynolds number $Re = 2$. It can be seen that the numerical results agree quite well with the analytical solutions.

The migration velocity under buoyant force only is provided by Refs. [19–22], considering both the viscous effect and inertial effect. After normalization, the migration velocity is as follows:

$$u_m = \frac{2}{3\left(2 + 3\frac{1}{R_v}\right)} \frac{\mathrm{Re}}{\mathrm{Fr}^2 K_{\mathrm{Is}}} \left(1 - \frac{1}{R_d}\right)\left(1 + \frac{1}{R_v}\right) \tag{10}$$

Here K_{Is} is the multiplier due to the inertial effect $K_{\mathrm{Is}} = 1 + 0.15\mathrm{Re}^{0.687}$. From Eq. (10) it is known that the migration velocity under buoyant effect depends on the viscosity ratio R_v and density ratio R_d, as well as Reynolds number Re and Froude number Fr. In Fig. 2(b) the numerical results are compared with the analytical solutions under different Froude numbers at $R_v = R_d = 20$ and low Reynolds number $Re = 2$. It can be seen that the numerical results agree quite well with the analytical solutions. The above comparisons prove the reliability of current numerical model.

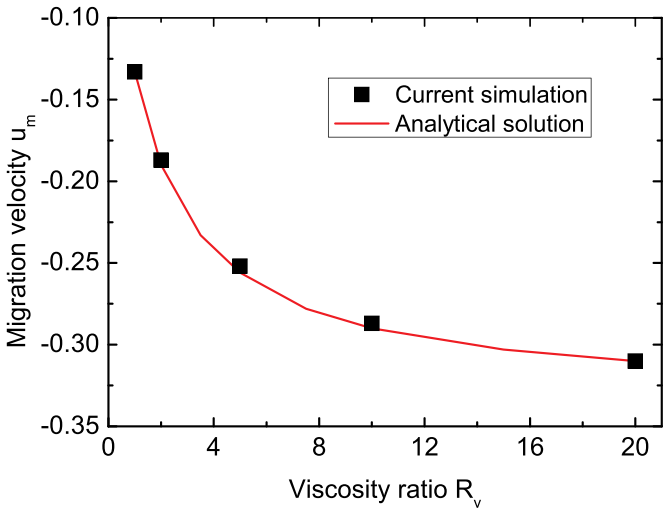

(a) Under thermal capillary force only

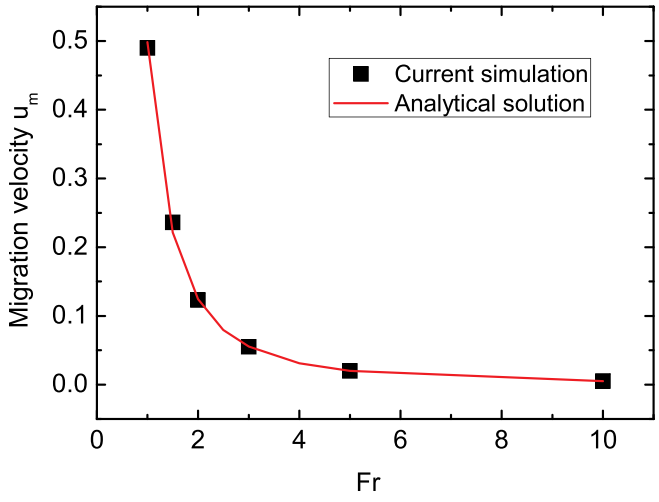

(b) Under buoyant force only

Fig. 2. Comparison of numerical results with analytical solution for bubble migration velocity at $\mathrm{Re} = 2$.

3.2. Bubble migration under thermal capillary effect or buoyant effect only

Fig. 3 shows the transient variation of bubble migration velocity under thermal capillary effect only at $Re = 2$ and $R_c = 1$. At the initial time the bubble is stagnant, with downward temperature gradient the upward tangential thermal capillary force is generated along the gas-liquid interface, because the surface tension decreases linearly with the temperature, i.e $\sigma_T < 0$. The force drives the gas from the bottom to the top of the bubble along the interface. In order to compensate the mass loss at the bottom, the gas will flow from the upper region to the lower region along the center of bubble. Therefore, the pressure at the higher region is higher than that at the lower region, the pressure drop will drive the bubble to move downward. With the increasing convection inside the bubble, the driving pressure drop will increase dramatically until the pressure drop is in balance with the viscous force and

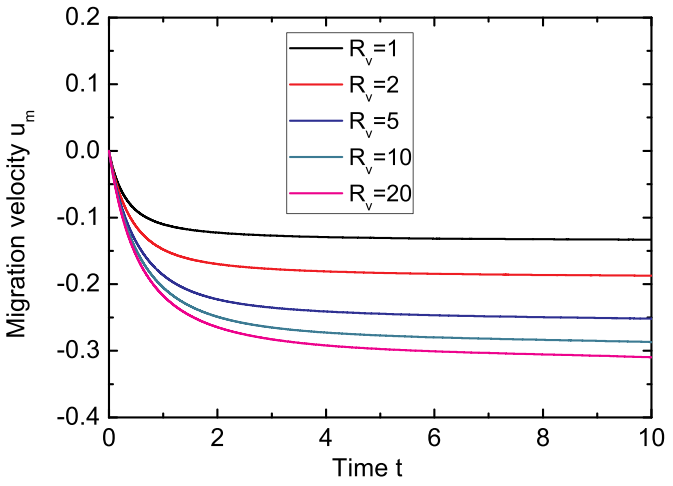

Fig. 3. Variation of migration velocities under thermal-capillary effect only at Re = 2.

thermal capillary force, then the bubble will reach the quasi-steady migration stage, as seen in Fig. 3. It can also be seen that with the increasing viscosity ratio, the magnitude of migration velocity is increased. At viscosity ratio $R_v = 1$, the steady migration velocity is −0.134, quite close to the analytical value of −0.133. When the viscosity ratio is increased to $R_v = 20$, the steady migration velocity is −0.311, also quite close to the analytical value of −0.310.

Fig. 4 shows the transient variation of bubble migration under buoyant effect only at $Re = 2$ and $R_v = 20$. The buoyant force is generated due to the density difference between the outer liquid and inner gas, here the density ratio is set at 20. According to the definition of Froude number in Eq. (8c), the larger Froude number means the smaller buoyant force. At the initial time the bubble is stagnant, then it will accelerate upward under the buoyant force. With the increasing migration velocity, the viscous force and inertial force will also increase. When the buoyant force is in balance with the viscous force and inertial force, the bubble will reach the quasi-stage stage. At $Fr = 1.0$, the steady upward migration velocity is 0.49, quite close to the analytical solution of 0.50. With the increasing Froude number, the buoyant force is decreased, resulting in the lower migration velocity, as seen in Fig. 4. At $Fr = 10$, the steady migration velocity is reduced to 0.005, identical to the analytical solution of 0.005.

As the Reynolds number is defined based on the velocity due to the thermal capillary effect in Eq. (1), the Reynolds number will not be very high. In the following studies, two typical Reynolds number $Re = 2$ and $Re = 50$ are adopted, which correspond to the cases when the viscous effect is significant and when the inertial effect is significant.

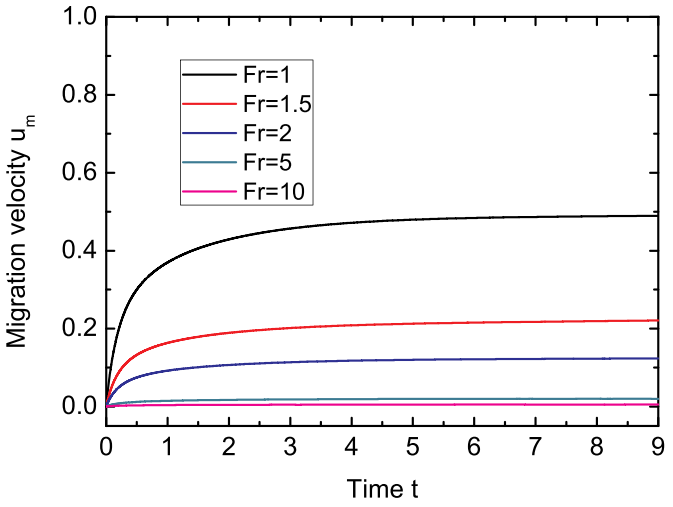

Fig. 4. Variation of migration velocities under buoyant effect only at Re = 2.

3.3. The effect of Froude number on bubble migration

3.3.1. Migration velocity

In Fig. 5 the effect of Froude number on the bubble migration velocity is shown at $Re = 2$ and $Re = 50$ respectively, here the density ratio and viscosity ratio and $R_d = R_v = 20$. At low Reynolds number $Re = 2$, it can be seen that the bubble will migrate upward at $Fr = 1$, while at large Froude numbers the bubble will migrate downward. Because at $Fr = 1$, the upward buoyant force is dominant over the thermal capillary force, while at high Froude number, the buoyant force is reduced, and the downward thermal capillary force becomes dominant, hence the bubble will migrate downward. Furthermore, with increasing Froude numbers the buoyant effect will be weakened further, leading to higher downward migration velocity. Therefore, the bubble migration direction and velocity can be directly manipulated by changing the Froude number.

It is noted that at low Reynolds number $Re = 2$ and Froude number

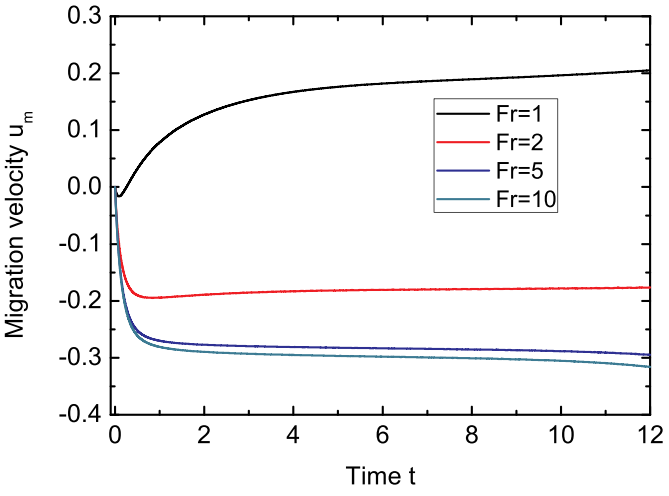

(a) Re = 2

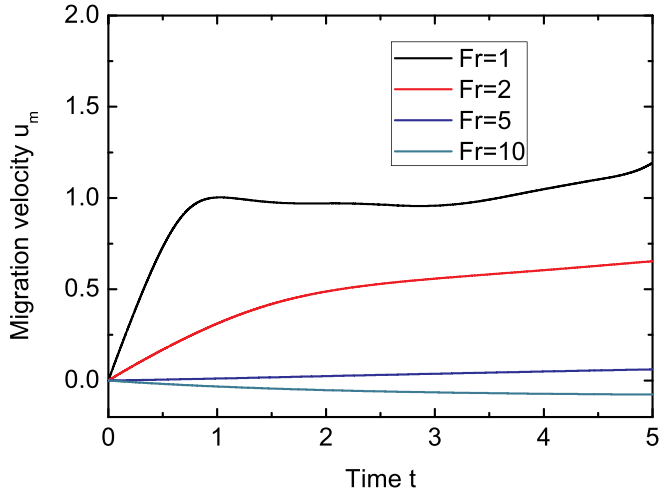

(b) Re = 50

Fig. 5. Effect of Fr number on migration velocity at $R_d = R_v = 20$.

$Fr = 2$, the bubble migration velocity is downward at around 0.18, while at high Reynolds number $Re = 50$, the bubble migration velocity is upward at around 0.65. It indicates that the Reynolds number has great effect on the bubble migration, the magnitude of migration velocity is higher at high Reynolds number $Re = 50$. At $Re = 2$ the thermal capillary effect is dominant, the heat is transferred mainly through heat conduction, the temperature distribution along the gas-liquid interface is quite non-uniform, leading to high thermal capillary force. However, at high Reynolds number $Re = 50$, the convection becomes stronger, the temperature distribution along the gas-liquid interface becomes more uniform, leading to low thermal capillary force. Because the buoyant force is not affected by the temperature, it will become dominant over the thermal capillary force, leading to the bubble to migrate upward. Therefore, the bubble migration can be manipulated by changing the Reynolds number.

3.3.2. Velocity and temperature field

Fig. 6 shows the velocity and temperature field under different Froude numbers at low Reynolds number $Re = 2$. It is noted that the velocities are all the relative velocities based on the steady bubble migration velocity. It can be found that at $Fr = 1$ the buoyant effect is dominant over the thermal capillary effect, the bubble will move upward, forming two vortices inside the bubble. In the meanwhile, two vortices also exit outside the bubble. Due to the upward bubble migration, the temperature field will deform upward. At $Fr = 1.4$ the buoyant effect is equivalent to the thermal capillary effect, there are still two large vortices inside the bubble, but the vortices outside the bubble disappear. Although the velocity inside the bubble is still large, the velocity far from the bubble is quite low, the temperature gradient is still similar to its initial field with the uniform gradient. At $Fr = 10$, the buoyant effect is negligible compared with the thermal capillary effect, the tangential velocity near the gas-liquid interface is upward due to the thermal capillary effect, while the velocity in the middle region of bubble is downward, which drives the bubble to migrate downward. The temperature field deforms downward due to the bubble migration.

3.3.3. Force analysis

The bubble migration velocity is determined by the inertial force, pressure drop, viscous force, thermal capillary force and the buoyant force, which are provided as follows:

$$\vec{F}_{\mathrm{In}} = \int_{\Omega} \rho^{*} \vec{u} \cdot \nabla \vec{u} \, dv \tag{11a}$$

$$\vec{F}_{P} = \int_{S} p \vec{n} \, ds \tag{11b}$$

$$\vec{F}_{\mathrm{Vis}} = \int_{S} \mu^{*} \left(\nabla \vec{u} + \nabla \vec{u}^{T} \right) \cdot \vec{n} \, ds \tag{11c}$$

$$\vec{F}_{\mathrm{Tc}} = \int_{S} \left(\frac{1 - \mathrm{Ma}T}{\mathrm{ReCa}} \kappa \vec{n} - \frac{\mathrm{Ma}}{\mathrm{ReCa}} \nabla_{s} T \right) ds \tag{11d}$$

$$\vec{F}_{B} = \int_{\Omega} \frac{(R_d - 1)}{R_d Fr^2} \vec{j} \, dv \tag{11e}$$

Here Ω is the bubble region, S is the gas-liquid interface. Fig. 7 shows the transient variations of different forces at $Fr = 1$, $Fr = 1.4$ and $Fr = 10$ respectively, corresponding to the bubble migration when buoyant force is dominant, buoyant force is equivalent with thermal capillary force, and thermal capillary force is dominant.

From Fig. 7(a) it can be seen that upon the imposition of temperature gradient, the thermal capillary force, buoyant force and pressure drop are generated, the buoyant force is quite larger than the thermal capillary force. Then with the increasing bubble migration velocity, the

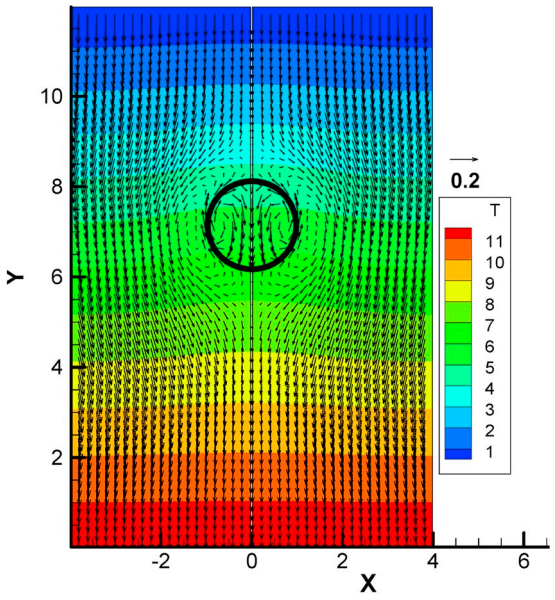

(a) Buoyant force is dominant (Fr = 1)

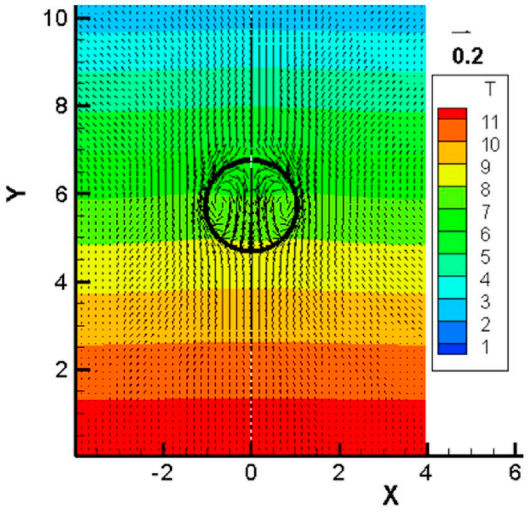

(b) Thermal capillary and buoyant force are equivalent (Fr = 1.4)

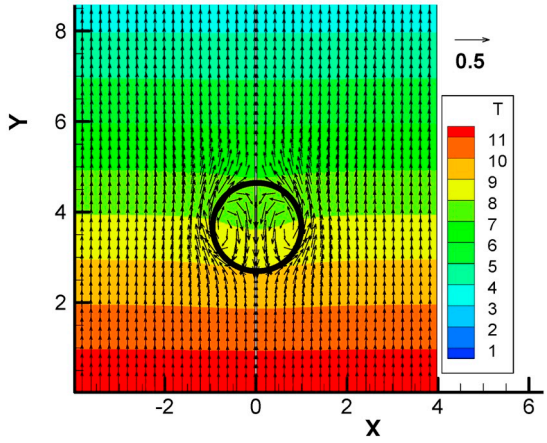

(c) Thermal-capillary force is dominant (Fr = 10)

Fig. 6. Flow and temperature fields with competing buoyant and thermal capillary effect at Re = 2, $R_d = 20$ and $R_v = 20$.

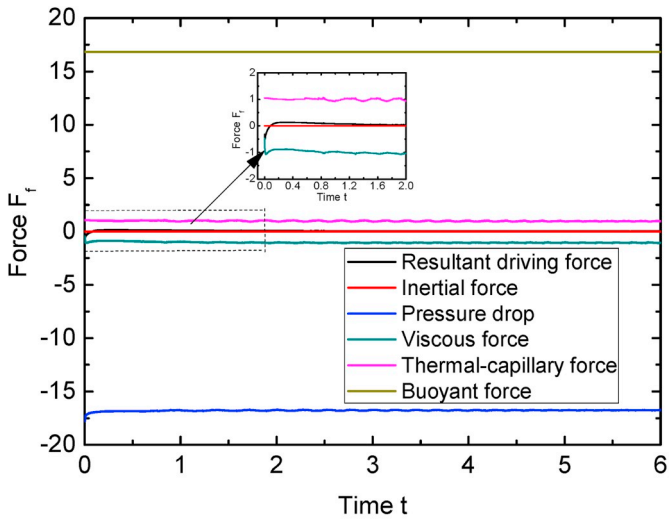

(a) Buoyant force dominant (Fr = 1)

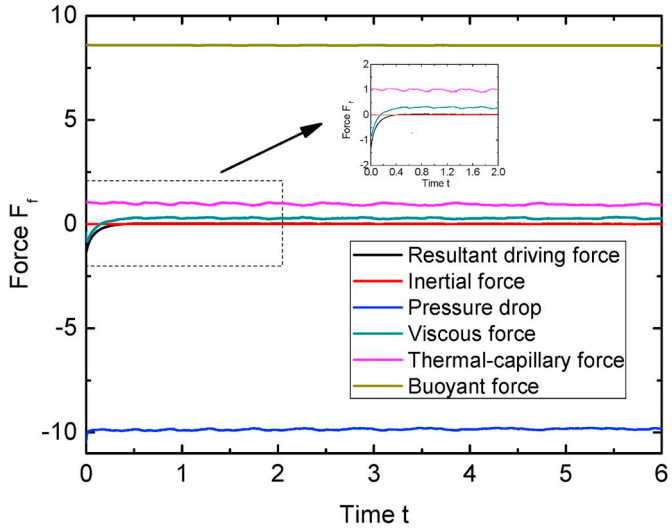

(b) Two forces are equivalent (Fr = 1.4)

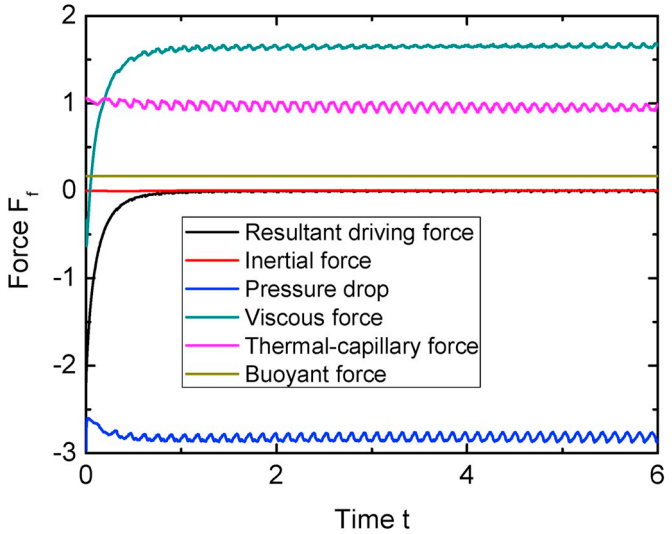

(c) Thermal-capillary dominant (Fr = 10)

Fig. 7. Transient variation of different forces on bubble migration at Re = 2, $R_d = 20$ and $R_v = 20$.

viscous force is generated, the resultant driving force becomes positive, driving the bubble to migrate upward. It is noted that the inertial force is negligible because it is viscous flow at low Reynolds numbers. After reaching the quasi-steady state, the resulting driving force becomes zero, all the forces are in balance, the pressure drop across the bubble is almost equivalent with the buoyant force, but in opposite direction, which means that the buoyant force is mainly balanced by the pressure drop. The pressure drop is mainly caused by the convection inside the bubble.

In Fig. 7(b) the buoyant effect is equivalent with the thermal capillary effect at $Fr = 1.4$, the resulting driving force approaches zero quickly, and the bubble reaches the quasi-steady state very soon. When Froude number is increased to 10, the thermal capillary effect becomes dominant over the buoyant effect, as seen in Fig. 7(c) the resultant driving force becomes negative, leading to the downward migration of the bubble. It is interesting to note that although the tangential thermal capillary force is upward along the interface, the bubble migrates downward, the only downward force is the pressure drop, which means that the driving force for bubble migration mainly comes from the pressure drop generated by the vortices inside the bubble. Due to the interaction between the flow field and temperature field, the bubble will deform during its migration, hence the forces acting on the bubble will fluctuate periodically, especially at high Froude number when the thermal capillary force is dominant.

3.4. Effect of Marangoni number on bubble migration

Fig. 8 shows the effect of Marangoni number on bubble migration velocity under different Froude numbers at $Re = 2$ and $Re = 50$ respectively. It can be seen that at low Reynolds number $Re = 2$ Marangoni number has little effect on bubble migration velocity at fixed Froude number. It is known that at $Fr = 1$ the buoyant effect is dominant over the thermal capillary effect, hence the Marangoni number has little effect on the bubble migration velocity. Furthermore, the characteristic velocity is defined based on the thermal capillary effect, hence even at $Fr = 2$ when the thermal capillary effect is dominant, the bubble migration velocity is independent of the Marangoni number, consistent with the analytical solution in Eq. (10). However, at high Reynolds number at $Re = 50$, the Marangoni number has significant effect on the bubble migration velocity, especially at the later stage of bubble migration. It can be found that with the increasing Marangoni number, the bubble migration velocities will be decreased. At high Reynolds numbers the convection will become stronger, which can transfer heat from the hot region to the cool region more effectively, leading to more uniform temperature field along the gas-liquid interface. Thus the thermal capillary effect will be reduced, the bubble migration velocity will be increased. It is noted that at $Fr = 2$ the bubble migration velocity can change from −0.2 at $Re = 2$ to 0.5–0.8 at $Re = 50$, it means that the direction and magnitude of bubble migration can be changed by varying Reynolds numbers.

3.5. Effect of Peclet number on migration velocity

Fig. 9 shows the effect of Peclet numbers on the bubble migration is shown at Re = 2 and $R_d = R_v = 20$. It is expected that with the increasing Peclet number, the convective heat transfer inside the bubble will become stronger, thus temperature distribution along the interface will become more uniform, the resultant thermal capillary effect will be weakened. For the buoyancy-dominant bubble migration at $Fr = 1$, due to the decreasing downward thermal-capillary effect, the upward migration of bubble will increase, especially after Peclet number is larger than 10. While for the thermocapillary-dominant bubble migration at $Fr = 2$, the downward bubble migration will be decreased.

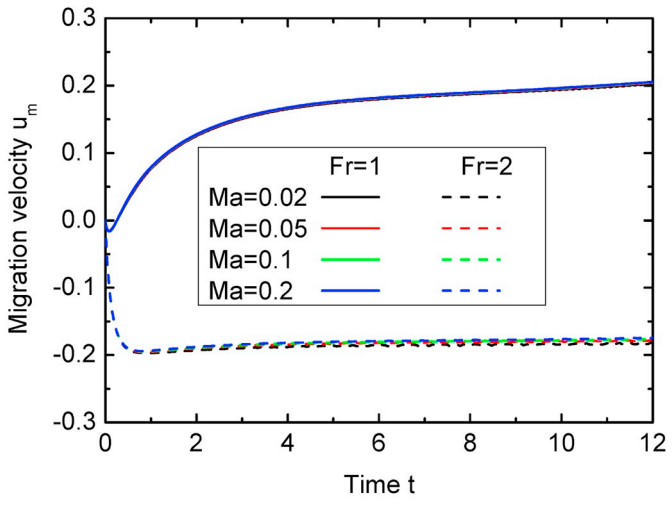

(a) Re = 2

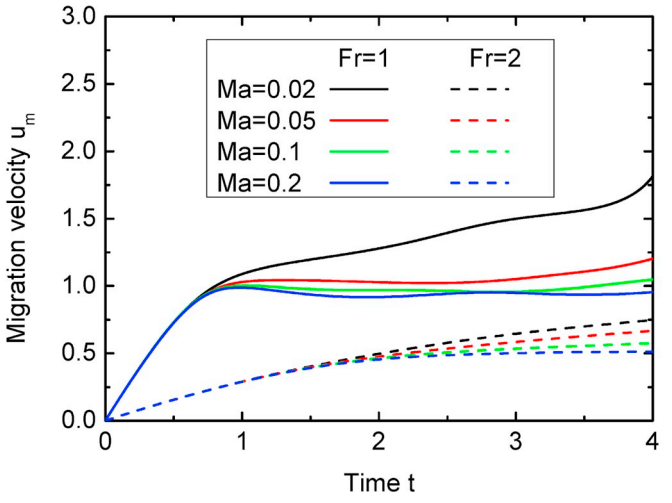

(b) Re = 50

Fig. 8. Effect of Marangoni number on migration velocity at R_d = 20, R_v = 20.

3.6. The effect of density ratio on bubble migration

The buoyant force is generated due to the density difference between the inner gas and the outer liquid, hence the density ratio has great effect on the bubble migration velocity. As seen in Fig. 10, at density ratio $R_d = 1$, there is no buoyant force, the bubble migration is driven by the thermal capillary effect only, hence Froude number has no effect on the bubble migration at $Re = 2$ and $Re = 50$. With the density ratio increases, the buoyant force will be increased, hence the upward buoyant force will overcome the thermal capillary force, the downward migration velocity will decrease, and the bubble will migrate upward at large density ratio. Due to the strong convective heat transfer at high Reynolds number, the thermal capillary effect will be reduced, at $Fr = 2$ the direction of migration velocity will change from the downward at $Re = 2$ to the upward at $Re = 50$ except at $R_d = 1$. At $Fr = 1$, the migration velocity is also increased significantly from $Re = 2$ to $Re = 50$.

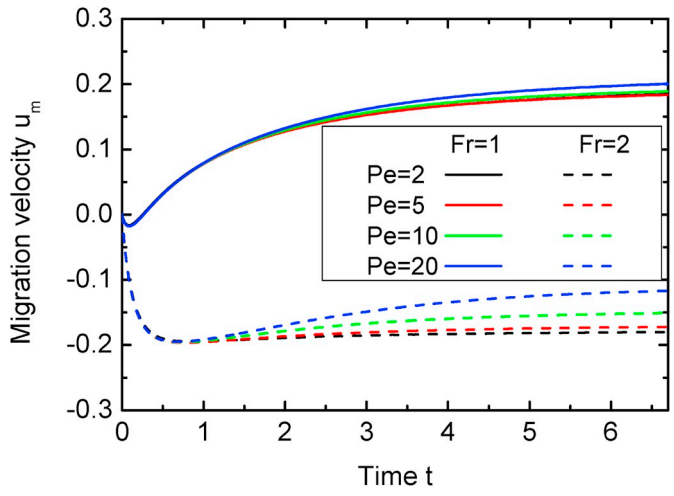

Fig. 9. Effect of Pe number on migration velocity at Re = 2 and $R_d = R_v = 20$.

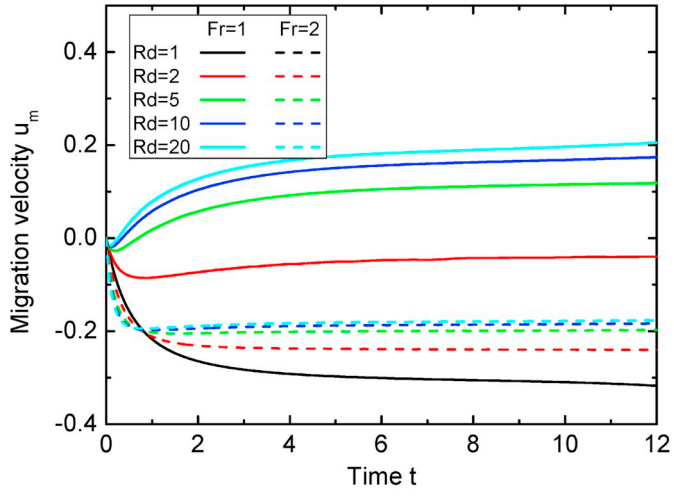

(a) Re = 2

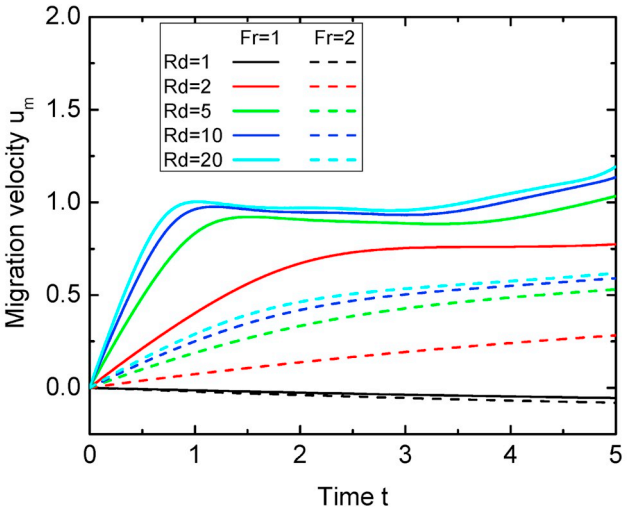

(b) Re = 50

Fig. 10. Effect of density ratio R_d on migration velocity at R_v = 20.

3.7. The effect of viscosity ratio on bubble migration

From Eq. (9) and Eq. (10) it is known that the viscosity ratio has both effects on the buoyancy-induced migration velocity and thermal capillarity-induced migration velocity. Fig. 11 shows the effect of viscosity ratio on the migration velocity under the combined effects of buoyancy and thermal capillarity at $Re = 2$ and $Re = 50$. It can be found that at low Reynolds number $Re = 2$, at $Fr = 1$ the buoyant force is dominant, the migration velocities are all upward and they decrease with the increasing viscosity ratio. While at $Fr = 2$, the thermal capillary effect is dominant, the migration velocities are all downward, and the magnitude of migration velocity increases with the increasing viscosity ratio. These results are consistent with the analytical solution in Eq. (9) and Eq. (10). However, at high Reynolds number $Re = 50$, the viscous effect becomes negligible compared with the inertial effect, hence the viscosity ratio has negligible effect on the migration velocity. Due to the weak thermal capillary effect at $Re = 50$, the directions of migration velocity change from downward at $Re = 2$ to upward, because it is mainly driven by the buoyant force.

3.8. The effect of thermal conductivity ratio on bubble migration

From Eq. (9) it is found that at low Reynolds number, the ratio of thermal conductivity can affect the bubble migration velocity due to thermal capillary effect, as seen in Fig. 12. At low Reynolds number $Re = 2$, at $Fr = 1$ the buoyant force is dominant over the thermal capillary force, with the increasing ratio of thermal conductivity, the upward migration velocity is decreased; At $Fr = 2$, the thermal capillary force is dominant, with the increasing ratio of thermal conductivity, the downward migration velocity is increased. However, at high Reynolds number $Re = 50$, the convective heat transfer becomes stronger than the heat conduction, the ratio of thermal conductivity has little effect on migration velocity. Due to the weak thermal capillary effect at $Re = 50$, the migration velocities at $Fr = 1$ and $Fr = 2$ are all upward, and the migration velocities at $Fr = 1$ are larger than those at $Fr = 2$ due to larger buoyant forces.

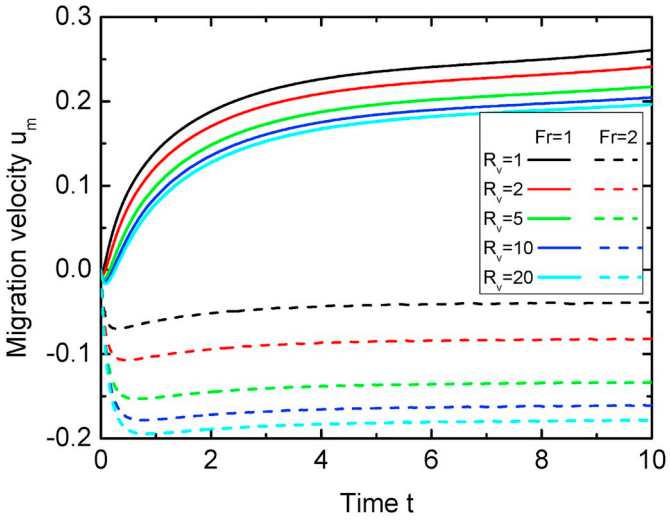

(a) Re = 2

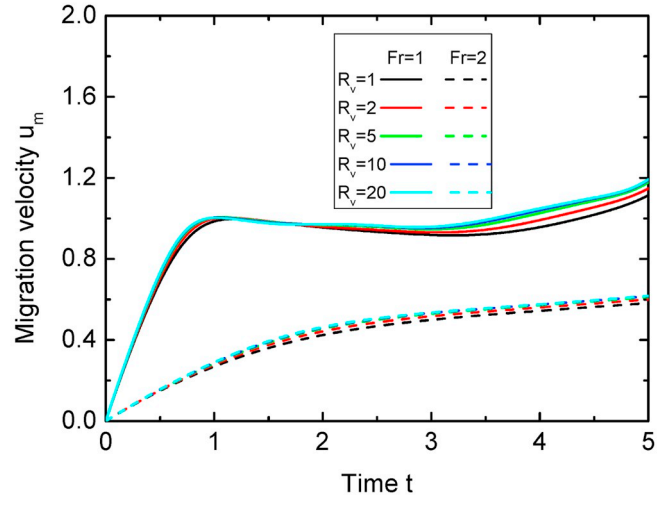

(b) Re = 50

Fig. 11. Effect of dynamic viscosity ratio R_v on migration velocity at $R_d = 20$.

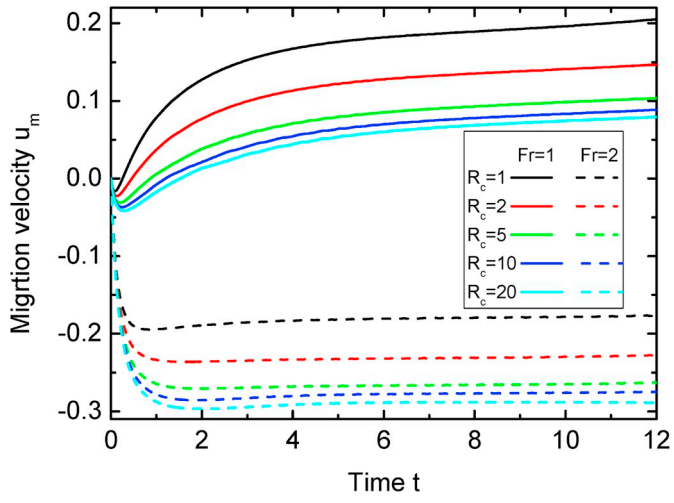

(a) Re = 2

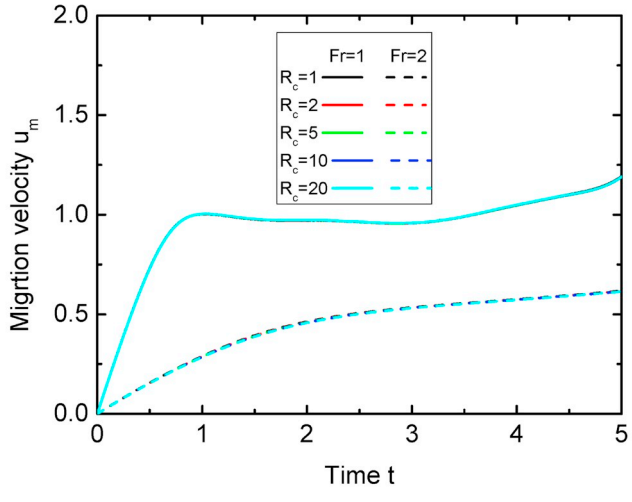

(b) Re = 50

Fig. 12. Effect of thermal conductivity ratio R_c on migration velocity at $R_d = 20$, $R_v = 20$.

4. Conclusions

The active manipulation of bubble can be achieved by the controlling the thermal capillarity and buoyancy under the critical condition when the thermal capillary effect and buoyant effect are equivalent. In this paper, the numerical model with high fidelity is built up with the axisymmetric level set method, the migration velocity and direction can be manipulated by adjusting the capillary, viscous, inertial and thermal capillary forces on the bubbles, as well as the physical properties. The following conclusions are drawn:

1. The direction and velocities of bubble migration is determined by the upward buoyant effect and downward thermal capillary effect. At low Froude number, the buoyant effect is dominant, leading to the upward bubble migration, while at high Froude number, the thermal capillary effect is dominant, leading to the downward bubble migration.
2. The Marangoni number has negligible effect on the bubble migration at low Reynolds or Peclet numbers. At high Reynolds or Peclet numbers, the increased Marangoni number can reduce the upward migration velocities due to the enhanced convective heat transfer.
3. Increasing the density ratio can increase the upward buoyant force due to the large density difference between the inner gas and the outer liquid.
4. At low Reynolds numbers, increasing the viscosity ratio and thermal conductivity ratio can increase the downward driving force due to enhanced thermal capillary effect. While at high Reynolds numbers, the above ratios have no effect on the driving force.

Acknowledgement

This work was financially supported by Natural Science Foundation of China (Grant No: 51436004, 51406050), Marie Curie European Fellowship (Grant No. 658437).

References

[1] R. Balasubramaniam, C.E. Lacy, G. Woniak, Thermocapillary migration of bubbles and drops at moderate values of the Marangoni number in reduced gravity, Phys. Fluids 8 (4) (1996) 872–880.
[2] R.S. Subramanian, R. Balasubramaniam, The Motion of Bubbles and Drops in Reduced Gravity, 0521496055, Cambridge University Press, 2001, 471.
[3] N.O. Young, J.S. Goldstein, M.J. Block, The motion of bubbles in a vertical temperature gradient, J. Fluid Mech. 6 (03) (1959) 350.
[4] R. Balasubramaniam, A.T. Chai, Thermocapillary migration of droplets: an exact solution for small marangoni numbers, J. Colloid Interface Sci. 119 (2) (1987) 531–538.
[5] A. Crespo, E. Migoya, F. Manuel, Thermocapillary migration of bubbles at large Reynolds numbers, Int. J. Multiph. Flow 24 (4) (1998) 685–692.
[6] A. Crespo, J. Jimenez-fernandez, Thermocapillary Migration of Bubbles: a Semi-analytical Solution for Large Marangoni Numbers, 8th European Symposium on Materials and Fluid Sciences in Microgravity, 1992, pp. 193–196.
[7] P.H. Hadland, R. Balasubramaniam, G. Wozniak, Thermocapillary migration of bubbles and drops at moderate to large Marangoni number and moderate Reynolds number in reduced gravity, Exp. Fluid 26 (3) (1999) 240–248.
[8] J.A. Szymczyk, G. Wozniak, J. Siekmann, On Marangoni bubble motion at higher Reynolds- and Marangoni-numbers under microgravity, Appl. Microgravity Technol. 1 (1) (1987) 27–29.
[9] R.L. Thompson, K.J. Dewitt, T.L. Labus, Marangoni bubble motion phenomenon in zero gravity, Chem. Eng. Commun. 5 (5–6) (1980) 299–314.
[10] J.A. Szymczyk, J. Siekmann, Numerical calculation of the thermocapillary motion of a bubble under microgravity, Chem. Eng. Commun. 69 (1988) 129–147.
[11] R. Balasubramaniam, J.E. Lavery, Numerical simulation of thermocapillary bubble migration under microgravity for large Reynolds and Marangoni numbers, Numer. Heat Transf. A 16 (2) (1989) 175–187.
[12] X. Ma, Numerical simulation of thermocapillary drop motion with internal circulation, Numer. Heat Transf. A 35 (3) (1999) 291–309.
[13] C. Zhang, P. Cheng, J. Cao, Mesoscale simulation of Marangoni convection about a vapor bubble in a liquid with temperature gradients under microgravity conditions, Int. Commun. Heat Mass Transf. 78 (2016) 295–303.
[14] J.F. Zhao, L. Zhang, Z.D. Li, W.T. Qin, Topological structure evolvement of flow and temperature fields in deformable drop Marangoni migration in microgravity, Int. J. Heat Mass Transf. 54 (2011) 4655–4663.
[15] B. Zhang, D. Liu, Y. Cheng, J. Xu, Y. Sui, Numerical investigation on spontaneous droplet/bubble migration under thermal radiation, Int. J. Therm. Sci. 129 (2018) 115–123.
[16] M.K. Tripathi, K.C. Sahu, G. Karapetsas, K. Sefiane, O.K. Matar, Non-isothermal bubble rise: non-monotonic dependence of surface tension on temperature, J. Fluid Mech. 763 (2015) 82–108.
[17] M. Balla, M.K. Tripathi, K.C. Sahu, G. Karapetsas, O.K. Matar, Non-isothermal bubble rise dynamics in a self-rewetting fluid: three-dimensional effects, J. Fluid Mech. 858 (2019) 689–713.
[18] M. Sussman, A.S. Almgren, J.B. Bell, et al., An adaptive level set approach for incompressible two-phase flows, J. Comput. Phys. 148 (1) (1999) 81–124.
[19] J.S. Hadamard, Mouvement permanent tent d'une sphere liquide et visquese dans un liquide visqueux, Comptes Rendus de I'Academie des Science 152 (1911) 1735–1738.
[20] W. Rybczynski, On the translatory of a fluid sphere in a viscous medium, Bull. Acad. Sci. Cracow Ser. A (1911) 40–46.
[21] L. Schiller, A. Naumann, Uber die grundlegende berechunung bei der schwekraft-aufbereitung, Z. Des. Vereines Dtsch. Ingenieure 44 (1933) 318–320.
[22] R. Kurimoto, K. Hayashi, A. Tomiyama, Terminal velocities of clean and fully-contaminated drops in vertical pipes, Int. J. Multiph. Flow 49 (2013) 8–23.